Vignetting Correction using Mutual Information submitted to ICCV '05

Seon Joo Kim and Marc Pollefeys
Department of Computer Science
University of North Carolina
Chapel Hill, NC 27599
{sjkim, marc}@cs.unc.edu

Abstract

In this paper, we propose a vignetting correction algorithm that does not require a reference image of a diffuse surface with uniform illumination. Acquiring such an image requires extreme care and special lighting equipments to ensure accuracy. Instead, we present an anti-vignetting algorithm that only requires few images of a normal scene and works independently of exposure and white balance changes. We achieve this goal by using a basic concept from information theory, mutual information (MI). Vignetting correction factors are estimated by maximizing the mutual information using the joint histogram of corresponding pixels in two images. The proposed approach is suitable for both rotating camera and moving camera. We show the performance of our algorithm by experiments using both simulated data and real images. Our method is especially useful for image mosaics, high dynamic range imaging, and radiometric calibration.

1. Introduction

What determines the brightness at a certain point in image? How is the image brightness related to scene brightness? Scene brightness can be defined by the term radiance which is the power per unit foreshortened area emitted into a unit solid angle by a surface [8]. After passing through the lens system, the power of radiant energy falling on the image plane is called the irradiance. Irradiance is then transformed to image brightness.

Recently, a lot of work has been done in finding the relationship between scene radiance and image intensity. The majority of research assumes linearity between radiance and irradiance, concentrating on estimating the radiometric response function which explains the nonlinear relationship between irradiance and image brightness [5, 6, 10, 11]. However, an important photometric distortion that spatially varies the amount of light hitting the image plane is not considered in most algorithms. This phenomenon of intensity falloff in the image periphery can have significant effect on images especially in image mosaics and in high dynamic range images.

1.1. Distortion Factors

The cosine-fourth law is one of the effects that is responsible for the lens falloff. It defines the relationship between radiance(L) and irradiance(E) using a simple camera model consisting of a thin lens and an image plane [8]. Eq. 1 shows that irradiance is proportional to radiance but it decreases as cosine-fourth of the angle α that a ray makes with the optical axis. In the equation, d is the radius of the lens and f denotes the distance between the lens and the image plane.

$$E = \frac{L\pi d^2 cos^4\alpha}{4f^2} \quad (1)$$

Most of cameras are designed to compensate the cosine-fourth effect [2] and the most dominant factor for irradiance falloff in the image periphery is due to a phenomenon called vignetting. Vignetting effect refers to the gradual fading-out of an image at points near its periphery due to the blocking of a part of the incident ray bundle by the effective size of aperture [18]. Effect of vignetting increases as the size of the aperture increases and vice versa. With a pinhole camera, there would be no vignetting.

Another phenomenon called pupil aberration has been described as a third important cause of fall in irradiance away form the image center in addition to the cosine-fourth law and vignetting [1]. Pupil aberration is caused due to nonlinear refraction of the rays which results in a significantly nonuniform light distribution across the aperture.

In this paper, we propose a new vignetting model that explains the observed irradiance falloff behavior rather than trying to physically model this radiometric distortion caused by combination of different factors. While there are multiple causes for the irradiance falloff, we will call the process of correcting this distortion vignetting correction since vi-

gnetting is the most dominant factor for the distortion and to conform with previous works.

1.2. Previous Work

Conventional methods for correcting vignetting involve taking a reference image of a non-specular object such as a paper with uniform white illumination. This reference image is then used to build correction LUT (Look Up Table) or to approximate parametric correction function. In the LUT method, a correction factor at each pixel is calculated by the following form[18] :

$$I_{LUT}(i,j) = I_{ref,max}/I_{ref}(i,j), \tag{2}$$

where I_{ref} is the reference image, $I_{ref,max}$ is the maximum intensity value of the reference image, and $I_{LUT}(i,j)$ is the correction value at pixel (i,j). After computing the LUT, images taken with the same setting can be corrected by multiplying each pixel with the corresponding value in the LUT.

In [2], Asada et al. proposed a camera model using variable cone that accounts for vignetting effects in zoom lens system. Parameters of the variable cone model were estimated by taking images of uniform radiance field. Yu et al. proposed using a hypercosine function to represent the pattern of the vignetting distortion for each scanline in [19]. They expanded their work to 2D hypercosine model in [18] and also introduced anti-vignetting method based on wavelet denoising and decimation. Other vignetting models include simple form using radial distance and focal length[16], third-order polynomial model[3], first order Taylor expansion[15], and empirical exponential function[4]. In [7] and [9], vignetting was used for camera calibration.

1.3. Goal and Outline of the paper

As mentioned, most existing vignetting correction methods require a reference image of a diffuse surface with uniform illumination. This process requires extreme care and special lighting equipments are necessary to ensure uniform illumination. While this illumination requirement was less strict for methods in [18, 19] which used normal indoor lighting, they still required images of uniform surface such as a white paper, attention to avoid casting a shadow on the surface, and their results relied heavily on proper acquisition of reference images.

In this paper, our goal is to correct vignetting without requiring an image of a diffuse surface with uniform lighting for reference. Instead, we present an anti-vignetting algorithm that only requires few images of a normal scene taken by rotating or translating the camera. We achieve this goal by using a basic concept from information theory, mutual information (MI). Parameters for vignetting model are estimated by maximizing the mutual information using the joint histogram of corresponding pixels in two images.

(a) (b) (c)

Figure 1: Joint histogram of a MR image with itself[13] - (a) rotated 0 degrees (b) rotated 2 degrees (c) rotated 5 degrees

This paper is organized as follows. Section 2 provides brief review of mutual information theory. Section 3 describes our vignetting correction method using mutual information. Section 4 presents experimental results and we discuss our proposed method and future works in section 5.

2. Mutual Information

Mutual information (MI) is a basic concept from information theory, measuring the statistical dependence between two random variables or the amount of information that one variable contains about the other [12]. With the work by Viola and Wells [17], mutual information has been used to solve many problems in computer vision such as pose estimation and object recognition. However, its primary use has been in image registration.

Defining A and B as two random variables with marginal probability distributions $p_A(a)$ and $p_B(b)$, and joint probability distribution $p_{AB}(a,b)$, mutual information $I(A,B)$ is defined by means of Kullback-Leibler measure as follows.

$$I(A,B) = \sum_{a,b} p_{AB}(a,b) log \frac{p_{AB}(a,b)}{p_A(a)p_B(b)} \tag{3}$$

We can interpret Eq.3 as measuring the degree of dependence of A and B by measuring the distance between the joint distribution $p_{AB}(a,b)$ and the distribution associated to the case of complete independence $p_A(a) \cdot p_B(b)$ [12].

We can also explain mutual information in terms of entropy :

$$\begin{aligned} I(A,B) &= H(A) - H(A|B) && (4)\\ &= H(B) - H(B|A) && (5)\\ &= H(A) + H(B) - H(A,B) && (6)\\ H(A) &= -\sum_a p_A(a) \log p_A(a) && (7)\\ H(A,B) &= -\sum_a \sum_b p_{AB}(a,b) \log p_{AB}(a,b) && (8) \end{aligned}$$

$$H(A|B) = -\sum_{a}\sum_{b} p_{AB}(a,b)\log p_{A|B}(a|b) \quad (9)$$

The entropy $H(A)$ is a measure of the amount of uncertainty about the random variable A. From Eq.4, mutual information I(A,B) is the reduction of uncertainty about A by the knowledge about another random variable B.

For image registration, image intensities a and b of corresponding pixels are considered to be random variables A and B. $p_{AB}(a,b)$ is computed by normalizing the joint histogram of overlapping regions of two images. $p_A(a)$ and $p_B(b)$ are also computed similarly by normalizing the histogram of joint regions for each image respectively. Then the registration parameters are estimated by finding parameters that maximizes the mutual information (Eq.3).

Fig.1 shows joint histograms of a MR image with itself [13] for different rotations which give good intuition about using mutual information for image registration. The first histogram is just a line since two images are identical. This is a case of perfect registration with maximum mutual information. As the image rotates, the images get more misaligned causing the joint histogram to spread more widely. The mutual information becomes smaller as the joint histogram disperses. We use this idea in our algorithm to correct vignetting which will be discussed in detail in the next section.

3. Vignetting Correction

3.1. Vignetting Model

The variable cone model proposed by Asada et al. [2] successfully predicts the vignetting distortion physically. However, the functional form of their model is difficult to implement due to inverse trigonometric functions in the model, and the model suffers from severely restricted field of view which makes the use of the model for practical application difficult [18]. The model requires focal length of the camera which also make this model impractical for our work. In [18, 19], empirical model using hypercosine was introduced. While it effectively models many cameras with smooth intensity falloff, the model was not suitable for cameras with sharp intensity falloff. Uyttendaele et al. proposed a simple model for vignetting in [16], but this model also requires focal length which makes it impractical for our method.

In this paper, we propose a new vignetting model that explains the observed irradiance falloff behavior rather than trying to physically model the vignetting effect. The function we use as the model is given in Eq. 10, where r is the normalized radial distance from the image center, N is the parameter for controlling the width of the intensity plateau, and α is the parameter responsible for the falloff rate (Fig.2). The vignetting correction factor would be the

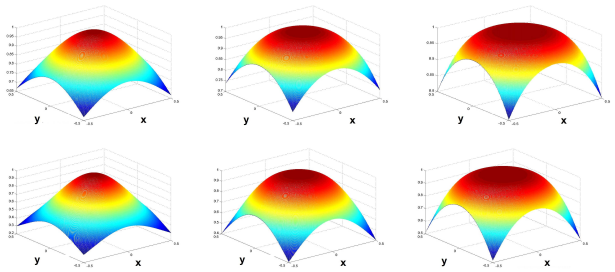

Figure 2: Proposed Vignetting Model. First row : α = 1, N = 2,3,4. Second row : α = 3, N = 2,3,4

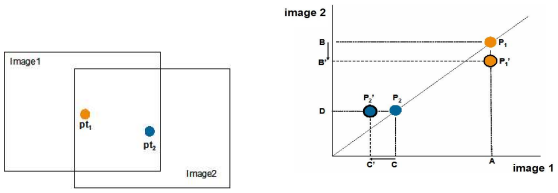

Figure 3: Effect of vignetting on joint histogram

inverse of f.

$$f(r) = \frac{1}{(1+r^N)^\alpha} \quad (10)$$

For an image I_0, vignetting is corrected (I) as follows :

$$I(r) = I_0(r)/f(r) \quad (11)$$

3.2. Anti-Vignetting by Maximizing Mutual Information

Consider the example shown in Fig.3. Two images are displaced by some amount and two points (pt1 and pt2) are located in the joint area between two images. Pt1 is in the center of image 1 and in the periphery of image 2. If images are not effected by vignetting, this point will have the same color in both images. If vignetting occurred, the color of the point in image 1 will stay the same since it is located in the center of the image, hence not affected by vignetting. However, the color of the point in image 2 will decrease from B to B' due to vignetting. So if we build a joint histogram of the corresponding points between this image pair, position at P_1' of the joint histogram will be incremented instead of P_1. Similarly for pt2, position at P_2' will be incremented rather then P_2.

The example shows how vignetting affects the joint histogram of the overlapping area of both images. The vignetting effect causes the joint histogram to spread more hence decreasing the mutual information, similar to the image registration example introduced in the previous section. The key of our algorithm is to find the parameters of our vignetting model that maximize the mutual information. In-

tuitively, it can be seen as a process of making the joint histogram more compact. Note that this idea holds independent of changes in exposure or white balance. Our method works also for a moving camera as far as correspondence can be found and the scene is mostly Lambertian.

Our algorithm for vignetting correction is summarized as follows:

1. Multiply each image with vignetting correction factor computed with initial parameters ($\mathbf{x} = [N, \alpha]$) (Eq. 10, Eq. 11).

2. Compute correspondence between two images. While there are multiple ways to compute correspondence between images such as computing homography, stereo matching, and optical flow, homography is used in all examples of this paper.

3. Compute joint histogram and marginal histograms from corresponding points : $h_{\mathbf{x}}(i_1, i_2)$, $h_{\mathbf{x}}(i_1)$, $h_{\mathbf{x}}(i_2)$.

4. Compute marginal and joint image intensity distributions, $p_{I_1,\mathbf{x}}(i_1)$, $p_{I_2,\mathbf{x}}(i_2)$, $p_{I_1 I_2,\mathbf{x}}(i_1, i_2)$

$$p_{I_1 I_2,\mathbf{x}}(i_1, i_2) = \frac{h_{\mathbf{x}}(i_1, i_2)}{\sum_{i_1}\sum_{i_2} h_{\mathbf{x}}(i_1, i_2)} \quad (12)$$

$$p_{I_1,\mathbf{x}}(i_1) = \frac{h_{\mathbf{x}}(i_1)}{\sum_{i_1} h_{\mathbf{x}}(i_1)} \quad (13)$$

$$p_{I_2,\mathbf{x}}(i_2) = \frac{h_{\mathbf{x}}(i_2)}{\sum_{i_2} h_{\mathbf{x}}(i_2)} \quad (14)$$

5. Estimate parameters (**x***) that maximize mutual information using Powell's optimization [12, 14].

$$I_{\mathbf{x}}(I_1, I_2) = \sum_{i_1}\sum_{i_2} p_{I_1 I_2,\mathbf{x}}(i_1, i_2) log \frac{p_{I_1 I_2,\mathbf{x}}(i_1, i_2)}{p_{I_1,\mathbf{x}}(i_1) p_{I_2,\mathbf{x}}(i_2)} \quad (15)$$

$$\mathbf{x}* = \arg\max_{\mathbf{x}}(I_{\mathbf{x}}(I_1, I_2)) \quad (16)$$

When aperture is fixed, the same model applies to a set of images that are used to correct vignetting. If aperture changes while taking pictures, different parameters should be used for each image. So, if we are using two images for the vignetting correction and aperture changes, we need to estimate 4 parameters, N and α for each image. More in general, in case of N-image panorama, we would need to estimate 2N parameters but instead of optimizing all parameters at once, we can work pairwise. For color images, we estimated parameters for each color channels separately.

4 Experiments

4.1 Synthetic Data

To evaluate our algorithm, we first performed experiments on synthetic images. By experimenting with synthetic images, we can first verify the use of mutual information for vignetting correction without worrying about correctness of the vignetting model.

Two images were generated from a larger image as shown in Fig.5. Vignetting effect and Gaussian noise (σ = 7) were added to each image. The first vignetting model we used for the simulation is shown in Fig.4 (a). As can be seen from Fig.5 (c), the effect of vignetting is more apparent in image mosaic. Using our algorithm, we were able to estimate the vignetting model accurately as can be seen in Fig.4 (b) and Fig.5 (g). Notice that after correcting the distortion, the image mosaic looks seamless and the joint histogram is much more compact.

We further tested our algorithm by increasing the intensity plateau of the models as shown in Fig.4 (d),(g). While we were able to get good estimation from both experiments, we observed that accuracy started to drop in the experiment with the model with shown in Fig.4 (g). This observation is apparent in mutual information plot in Fig.4. While the first model results in a sharp peak in the mutual information plot, the peak blends as the width of the intensity plateau of vignetting grows, resulting in decrease of accuracy. This is result of lack of information since area affected by vignetting is very small.

4.2. Real Data

To verify the overall performance of our algorithm, we applied our method to real images. For the first experiment (Fig.6), two images were taken with a Sony DSC-P9 camera. Vignetting effect is clearly seen from the image panorama built by aligning the image pair. After applying our correction method, vignetting effect is vastly removed (Fig.6, second row). However, the vignetting correction is not perfect as there are some vignetting effects left especially in the dark region under the board in the picture.

Second experiment was done using images downloaded from a website (Fig.6). Again, while not perfect, vignetting effect is vastly removed. This example shows one of the advantages of our algorithm. We do not have to pre-calibrate vignetting factors using a reference image. Instead, we just use images used for application directly.

5. Conclusion

In this paper, we have proposed a novel method for vignetting correction. The key advantage of our method over

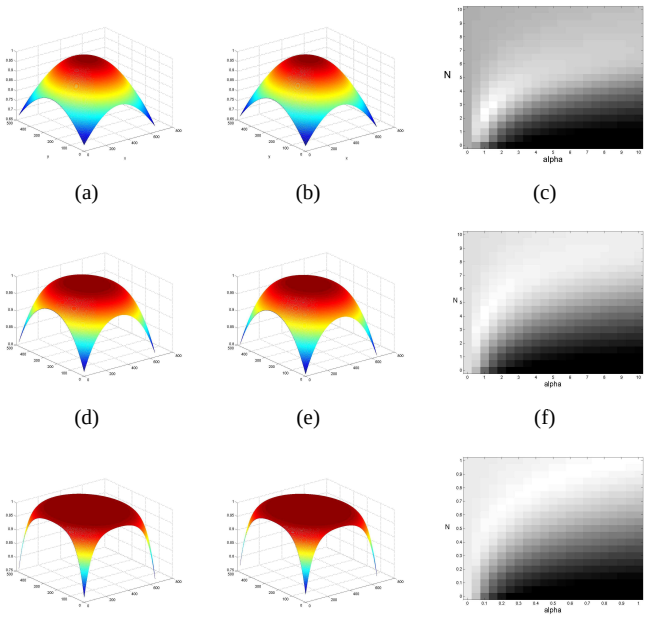

(a) (b) (c)

(d) (e) (f)

(g) (h) (i)

Figure 4: Synthetic Experiment (a),(d),(g) Model used for simulation1 (N = 2.5, α = 1.1),(N = 4.2, α = 1.0),(N = 9.5, α = 7.5) (b),(e),(h) Model estimated with our algorithm (N = 2.52, α = 1.12), (N = 4.15, α = 0.99),(N = 9.3, α = 6.7) (c),(f),(i) Mutual information with changes in parameters specified by grayscale value

previous methods is that we do not require a reference image of a diffuse surface with uniform illumination which requires extreme care and special lighting equipments to ensure accuracy. Instead, our algorithm only requires a pair of images to correct vignetting and it is independent of exposure and white balance changes. The performance of the proposed method was verified by experiments with synthetic and real data.

The synthetic experiments showed that our algorithm is well suited for vignetting correction. While the results from real images also showed vast improvement in getting vignetting free images, there is still room for improvement. At this point we apply our algorithm directly to image brightness rather than to image irradiance (Eq.11). Basic underlying assumption is that the relationship between irradiance and image brightness is linear which is seldom the case. Because our approach is more sensitive to brighter pixels as they are more affected by vignetting (in absolute terms), for nonlinear response our approach tends to fit the shape of the upper part of the response curve providing better results for brighter image region and not perfectly compensating the darker region (see joint histograms in Fig.7). To achieve more accurate results, image brightness should be transformed to image irradiance using radiometric response function [5, 6, 10, 11]. We plan to work on combining the proposed method with radiometric response function estimation in the near future. The proposed approach could be very helpful for radiometric calibration, high dynamic range imaging, and image mosaics. We also plan to enhance the proposed algorithm to deal with images with large plateau and sharp intensity fall-off better.

References

[1] M. Aggarwal, H. Hua, and N. Ahuja, "On Cosine-fourth and Vignetting Effects in Real Lenses", Proc. IEEE Int. Conf. on Computer Vision, July 2001

[2] N. Asada, A. Amano, and M. Baba, "Photometric Calibration of Zoom Lens Systems", Proc. IEEE Int. Conf. on Pattern Recognition, pp 186-190, Aug. 1996

[3] C. M. Bastuscheck, "Correction of Video camera response using digital techniques", J. of Optical Engineering, vol. 26, no. 12, pp.1257-1262

[4] Y. P. Chen and B. K. Mudunuri, "An anti-vignetting technique for superwide field of view mosaicked images", J. of Imaging Technology, vol. 12, no. 5, pp. 293-295, 1986

[5] P. Debevec and J. Malik, "Recovering High Dynamic Range Radiance Maps from Photographs", Computer Graphics, Proc. SIGGRAPH'97, pp. 369-378, 1997.

[6] M. D. Grossberg and S. K. Nayar, "Modeling the Space of Camera Response Functions", IEEE Transaction on Pattern

Analysis and Machine Intelligence, Vol. 26, No. 10, Oct. 2004

[7] M. D. Grossberg and S. K. Nayar, ”A General Imaging Model and a Method for Finding its Parameters”, Proc. IEEE Int. Conf. on Computer Vision, July. 2001

[8] B. K. P. Horn, ”Robot Vision’, The MIT Press, Cambridge, Mass., 1986

[9] S. B. Kang and R. Weiss, ”Can we calibrate a camera using an image of a flat, textureless Lambertian surface?”, Proc. of the 6th European Conference on Computer Vision, July, 2000

[10] S. J. Kim and M. Pollefeys, ”Radiometric Alignment of Image Sequences”, Proc. IEEE Conference on Computer Vision and Pattern Recognition, June 2004

[11] S. Lin, J. Gu, S. Yamazaki, and H. Shum, ”Radiometric Calibration from a Single Image”, Proc. IEEE Conference on Computer Vision and Pattern Recognition, June 2004

[12] F. Maes, A. Collignon, D. Vandermeulen, G. Marchal, and P. Suetens, ”Multimodality Image Registration by Maximization of Mutual Information”, IEEE Transaction on Medical Imaging, Vol. 16, No. 2, April 1997

[13] J. P. W. Pluim, J. B. A. Maintz, and M. A. Viergever, ”Mutual information based registration of medical images: a survey”, IEEE Transaction on Medical Imaging, Vol. 22, No.8, Aug. 2003

[14] W. H. Press, B. P. Flannery, S. A. Teukolsky, and W. T. Vetterling, ”Numerical Recipes in C, 2nd ed.”, Cambridge, U. K.: Cambridge Univ. Press, 1992, ch. 10, pp 412-419

[15] A. A. Sawchuk, ”Real-time correction of intensity nonlinearities in imaging systems”, IEEE Transactions on Computers, vol. 26, no.1, pp. 34-39, 1977

[16] M. Uyttendaele, A. Criminisi, S. B. Kang, S. Winder, R. Hartley, Richard Szeliski, ”Image-Based Interactive Exploration of Real-World Environments”, IEEE Computer Graphics and Applications, Vol. 24, No. 3, June 2004

[17] P. Viola and W. M. Wells III, ”Alignment by Maximization of Mutual Information”, International Journal of Computer Vision, vol. 24(2), pp. 137-154, Sept. 1997

[18] W. Yu, ”Practical Anti-vignetting Methods for Digital Cameras”, IEEE Transactions on Consumer Electronics, Vol. 50, No. 4, Nov. 2004

[19] W. Yu, Y. Chung, and J. Soh, ”Vignetting Distortion Correction Method for High Quality Digital Imaging”, Proc. IEEE Int. Conf. on Pattern Recognition, Aug. 2004

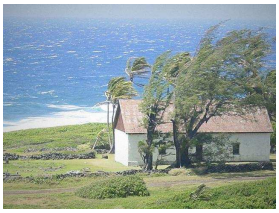

(a) Synthetic image : N = 2.5, α = 1.1, Gaussian noise with $\sigma = 7$

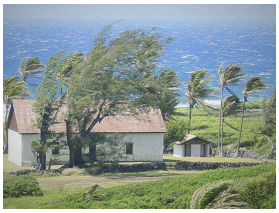

(b) Synthetic image

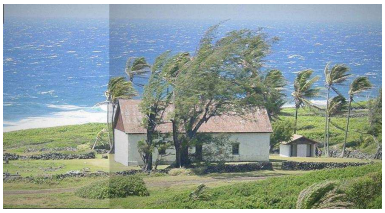

(c) Image mosaic of (a),(b)

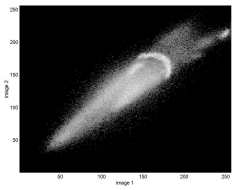

(d) Joint histogram of (a),(b)

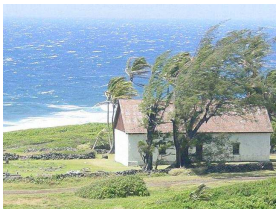

(e) Vignetting corrected image of (a)

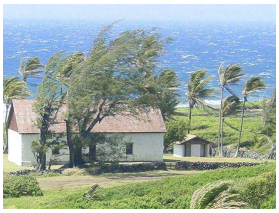

(f) Vignetting corrected image of (b)

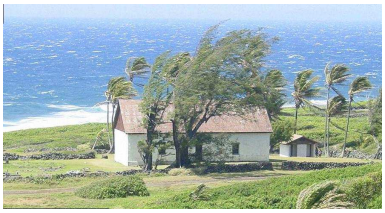

(g) Image mosaic of (d),(e)

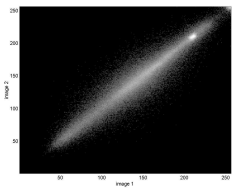

(h) Joint histogram of (d),(e)

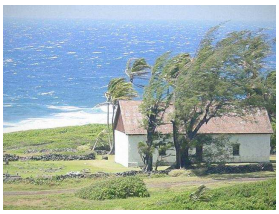

(i) Synthetic image : N = 4.2, α = 1.0, Gaussian noise with $\sigma = 7$

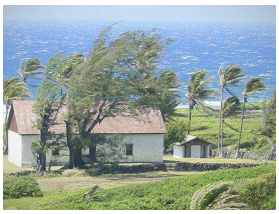

(j)

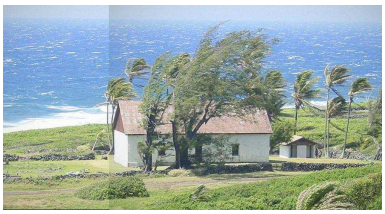

(k)

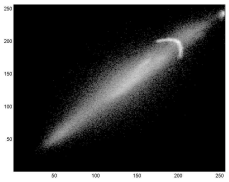

(l)

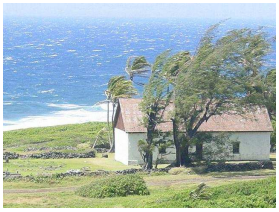

(m)

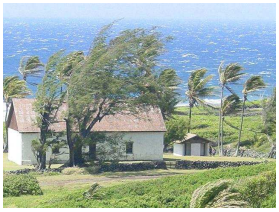

(n)

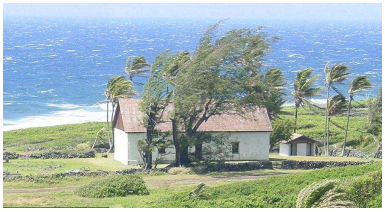

(o)

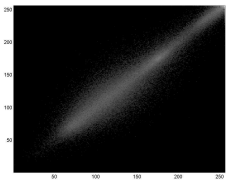

(p)

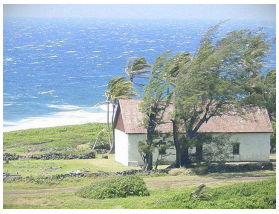

(q) Synthetic image : N = 9.5, α = 7.5, Gaussian noise with $\sigma = 7$

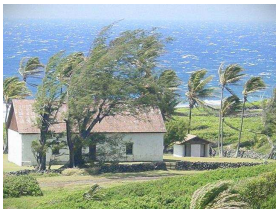

(r)

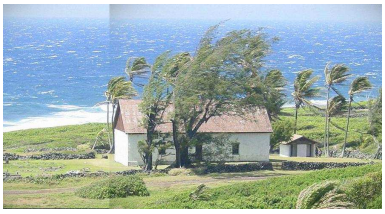

(s)

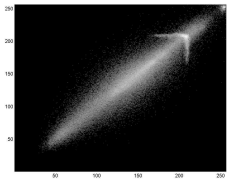

(t)

(u)

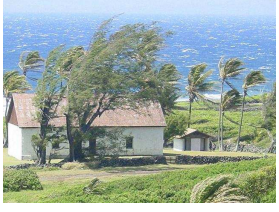

(v)

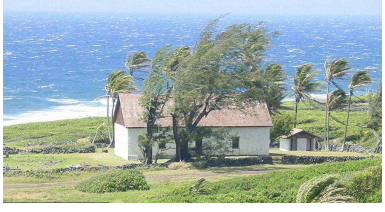

(w)

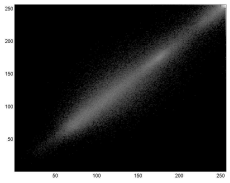

(x)

Figure 5: Experiment with synthetic images

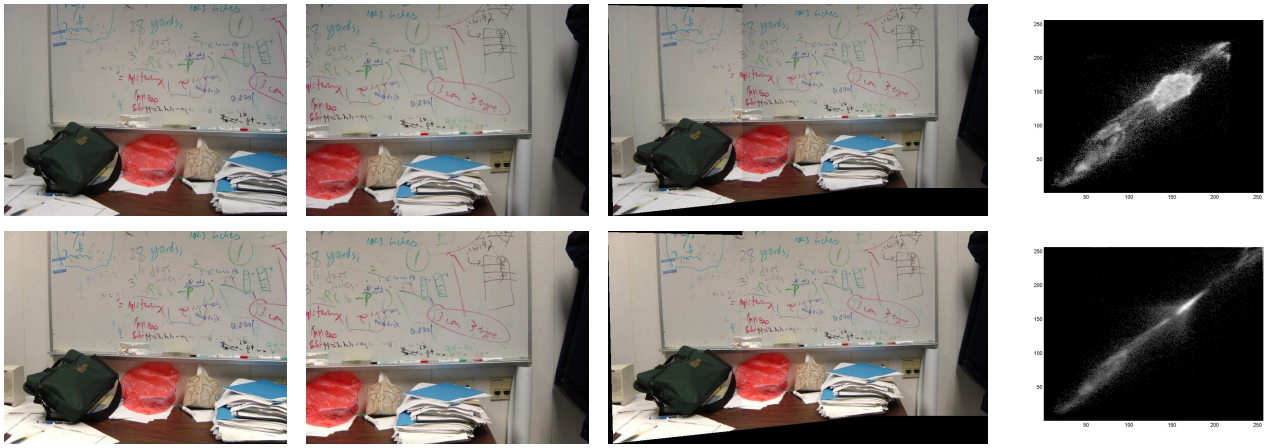

Figure 6: Experiment with real images . First row : images taken with Sony DSC-P9. Second row : Vignetting corrected images. Reviewers, please look at the images through monitors rather than images printed.

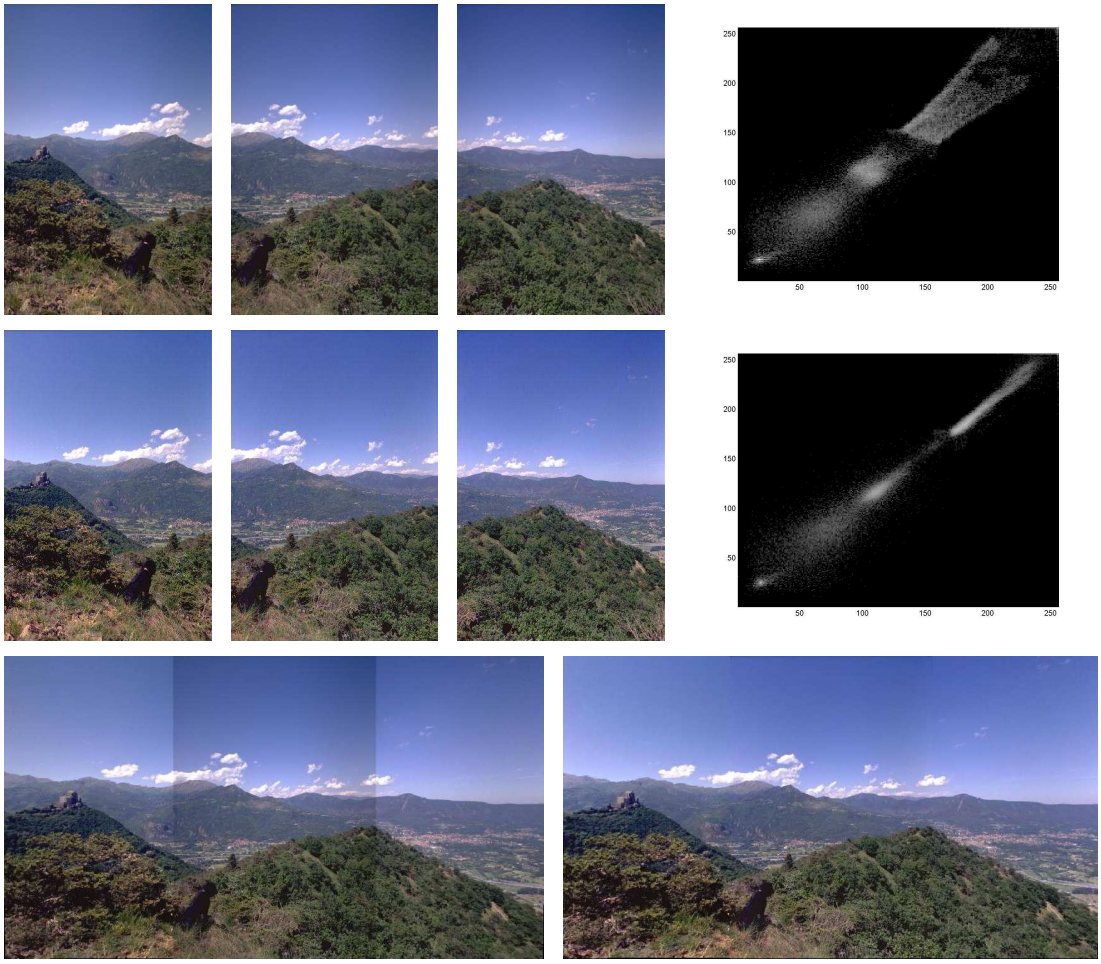

Figure 7: Experiment with real images. First row : images from http://www.fsoft.it/Imaging/Vignetting.htm and joint histogram of green channel. Second row : Vignetting corrected images and joint histogram. Third row : Original image panorama and vignetting corrected image panorama. Reviewers, please look at the images through monitors rather than images printed.